Structural basis of the cross-reaction between an antibody to the *Trypanosoma cruzi* ribosomal P2β protein and the human β_1 adrenergic receptor

C. Smulski,* V. Labovsky,* G. Levy,* M. Hontebeyrie,† J. Hoebeke,‡ M. J. Levin*,§,1

*Laboratorio de Biología Molecular de la Enfermedad de Chagas (LaBMECh), Instituto de Investigaciones en Ingeniería Genética y Biología Molecular (INGEBI), National Research Council (CONICET), Buenos Aires, Argentina; Institut Pasteur, Paris, France; ‡UPR 9021 "Immunologie et Chimie Thérapeutiques" du C.N.R.S., Institut de Biologie Moleculaire et Cellulaire (IBMC), Strasbourg, France; and §Institut Cochin, Département Maladies Infectieuses, INSERM U567, Paris, France

ABSTRACT **Antibodies from patients with Chagas heart disease and monoclonal antibodies (or mAb) to the carboxy-terminal end (B cell epitope R13) of the ribosomal P2β protein of *Trypanosoma cruzi* (TcP2β) cross-react with the β_1 adrenergic receptor (β_1-AR). Two single-chain Fv fragments (scFv) C5 and B7 derived from the variable regions of the anti-R13 mAb 17.2 were expressed. scFv C5 was a dimer and bound to TcP2β with an affinity of K_d = 8 nM, whereas scFv B7 was monomeric and had less affinity than scFv C5 for TcP2β, K_d = 46 nM. The affinity constant of scFv C5 to the second extracellular loop of the human β_1-AR was of 10 μM. Moreover, scFv C5 induced an increase in cAMP levels of CHO-K cells transfected with the human β_1-AR; scFv B7 had no effect but blocked isoproterenol stimulation. The agonist-like activity of scFv C5 and the antagonist activity of scFv B7 were both confirmed *in vivo* on heart beating frequency after their passive transfer to mice. Molecular modeling of the variable region of mAb 17.2 indicated which amino acids were likely to be involved in recognizing both peptide EDDDMGFGLF, derived from the R13 epitope of TcP2β, and peptide ESDEARRCYN from the second extracellular loop of the human β_1-AR. It is plausible that the recently described cross-reaction of mAb 17.2 with rhodopsin can also be explained by this model. The physiological effects of this type of anti-*T. cruzi* antibodies may increase the liability of patients with Chagas disease.—Smulski, C., Labovsky, V., Levy, G., Hontebeyrie, M., Hoebeke, J., Levin, M. J. Structural basis of the cross-reaction between an antibody to the *Trypanosoma cruzi* ribosomal P2β protein and the human β_1 adrenergic receptor. *FASEB J.* 20, 1396–1406 (2006)**

Key Words: ribosomal P proteins · single-chain Fv fragments (scFv) · paratope-epitope modeling

Chagas disease, caused by the protozoan parasite *Trypanosoma cruzi*, affects 18–20 million people in Latin America. The most severe manifestation of this infection is chronic Chagas heart disease (cChHD) (1). Its slow evolving nature, together with scarcity of parasites at the lesion site, as monitored in mild forms of the disease, suggests an autoimmune component in its pathogenesis (1, 2). Supporting evidence for this hypothesis is the presence of circulating anti-parasite antibodies (Abs) with agonist-like properties on cardiac autonomic receptors in these patients (3–5). Our studies with a cohort of patients with Chagas heart disease have demonstrated a correlation between the presence of Abs that stimulate the β_1 adrenergic receptor (β_1-AR) and the incidence of ventricular arrhythmia, as well as the occurrence of M_2 acetylcholine receptor (M_2-AchR) -stimulating Abs in patients with sinus node dysfunction (6, 7). We have hypothesized that these cardiac receptor-stimulating activities are the expression of a bystander effect of Abs primarily directed against parasite structures (8, 9). This assumption is based on the fact that Abs against the C-terminal end of the ribosomal P2β protein of *T. cruzi* (TcP2β) were able to cross-react with the β_1-AR. This effect has been attributed to the highly antigenic acidic epitope present at the C-terminal end of TcP2β named R13, EEEDDDMGFGLFD, which bears similarity to an acidic motif, AESDE, on the second extracellular loop of the receptor (8, 9).

Mice immunized with the recombinant TcP2β protein that raised a strong response against R13 developed lethal supraventricular tachycardia, suggesting that the high anti-R13 antibody (Ab) titers were responsible for the sustained β_1-AR stimulation of the heart. In addition, recent immunization experiments have demonstrated that recognition of the E residue in position 3 of R13 mediates the ability of anti-R13 Abs to react with the AESDE motif of the β_1-AR (9). These findings have been further confirmed by the generation of an anti-R13 mAb 17.2 that possesses strong

[1]Correspondence: LaBMECh, Instituto de Investigaciones en Ingeniería Genética y Biología Molecular (INGEBI-CONICET), Vta. de Obligado 2490, C1428ADN, Ciudad de Buenos Aires, Argentina. E-mail: mlevin@dna.uba.ar

doi: 10.1096/fj.05-5699com

0892-6638/06/0020-1396 © FASEB

β_1-AR stimulatory activity (10). The aim of the present study was to elucidate the structural basis of the cross-reactivity of Abs directed against the ribosomal TcP2β protein with the second extracellular loop of the β_1-AR and to demonstrate the ability of anti-TcP2β Abs to induce cardiac symptoms after passive immunization. To accomplish these objectives, we derived four different single-chain Fv fragments (scFv) from mAb 17.2 that were cloned, sequenced, and expressed in *Escherichia coli*. The immunochemical, pharmacological, and physiological properties of each scFv were tested. Results showed that the R13 epitope was able to induce an Ab that recognizes the second extracellular loop of the β_1-AR. When these Abs were passively transferred into mice, they induced ventricular arrhythmia. These results stress the role the parasite plays in the generation of an autoimmune response that has been long known to exist in Chagas disease.

MATERIALS AND METHODS

ScFv construction

Total RNA was isolated from mAb 17.2 expressing hybridoma cells using the RNeasy kit (Qiagen, Valencia, CA, USA). cDNA synthesis was performed with Moloney murine leukemia virus reverse transcriptase, using random hexamers as primers (Promega, Madison, WI, USA). Polymerase chain reaction (PCR) amplification was carried out using Pfu polymerase (Stratagene, La Jolla, CA, USA). The heavy and light chain variable regions (VH and VL) were amplified in a two-step PCR using the following primers: VHF (5′-GAAGTGCAGCTCGAGGAGTCTGG-3′), VHR (5′-AGAGACAGTGACCAGAGTCCCTTGGCC-3′), VLF (5′-GAGCTCGTGATGACACAGTCTCCA-3′), and VLR (5′-CCGTTTTATTTCCAGCTTGGTCCC-3′). The linker and restriction sites sequences were added in a second overlap PCR using the following primers: 17.2 Sfi (5′-CATGCCATGACTCGCGGCCCAGCCGGCCATGGCCGAAGTGCAGCTCGAGGAGTCTGG–3′), 17.2 LBSH (5′-GCCACCCAGCCCGCCAGAGACAGTGACCAGAGTCCCTTGGCC–3′), 17.2 LFSH (5′-GGCGGGTCGGGTGGCGAGCTCGTGATGACACAGTCTCC–3′), 17.2 LBLG (5′-CCCCCGCCGCCCGACCCGCCACCTCCAGAGACAGTGACCAGAGTCCCTTGGCC–3′), 17.2 LFLG (5′-GGCGGGTCGGGCGGCGGGGGATCGGGTGGCGGAGGGTCGGAGCTCGTGATGACACAGTCTCC–3′), and NOTVKFOR2 (5′-GATATGAGATACTGCGGCCGCCCGTTTTATTTCCAGCTTGGTCCC–3′) for the VH-VL short (SH) and long (LG) linker cassettes. Primers 17.2 *Sfi*VL (5′-CATGCCATGACTCGCGGCCCAGCCGGCCATGGCCGAGCTCGTGATGACACAGTCTCC–3′), 17.2 LBSH VL (5′-GCCACCCGACCCGCCCCGTTTTATTTCCAGCTTGGTCCC–3′), 17.2 LFSH VH (5′-GGCGGGTCGGGTGGCGAAGTGCAGCTCGAGGAGTCTGG–3′), 17.2 LBLG VL (5′-CCCCCGCCGCCCGACCCGCCACCTCCCCGTTTTATTTCCAGCTTGGTCCC–3′), 17.2 LFLG VH (5′-GGCGGGTCGGGCGGCGGGGGATCGGGTGGCGGAGGGTCGGAAGTGCAGCTCGAGGAGTCTGG–3′), and NOTVHFOR2 (5′-GATATGAGATACTGCGGCCGCAGAGACAGTGACCAGAGTCCCTTGGCC–3′) were used for the VL-VH short (SH) and long (LG) linker cassettes. The PCR products were cloned into the *Sfi*I and *Not*I sites of the prokaryotic phagemid pHen II vector (see Fig. 2*A*). The multiple cloning site (MCS) is preceded by a pelB leader sequence, followed by a six-histidine tag, a c-*myc* epitope, an amber stop codon, and the p3 gene (phage M13 capsid) fused to the C-terminal region. This allowed either selection of reactive phages or production of soluble recombinant Abs (11). Sequencing was carried out on a MegaBACE 500 instrument (Amersham Pharmacia, Little Chalfont, UK). Four different scFvs were selected for further study: C5 (VH-VL short linker), B7 (VH-VL long linker), F4 (VL-VH short linker), and G12 (VL-VH long linker).

Bacterial expression and purification of scFv

Bacterial expression of the recombinant scFv proteins and extraction of soluble periplasmic protein were performed as described in ref 12. The periplasmic extracts were centrifuged at 10,000 *g*, and the supernatants were filtered on 0.45 μm membrane and extensively dialyzed against PBS-I (50 mM Na_2HPO_4, 300 mM NaCl, 20 mM imidazole). Thereafter, extracts were incubated for 1 h at 4°C with 500 μl of nickel-nitrilotriacetic acid-agarose beads (Qiagen, Valencia, CA, USA) and washed with PBS-I buffer. The recombinant proteins were eluted with 1 ml of PBS-I supplemented with 500 mM imidazole and immediately dialyzed against PBS. The total protein concentration of the purified scFvs was determined using Bradford reagent (Bio-Rad, Hercules, CA, USA) and measuring absorbance at 280 nm. The extinction coefficient was determined using the Expasy protparam tool available on the web (www.expasy.org/tools/protparam.html).

Gel electrophoresis and Western blot analysis

SDS-PAGE analysis was performed as a standard procedure using 12% acrylamide gels, followed by staining with Coomassie brilliant blue or immunoblotting. For Western blot analysis, proteins were transferred from gels onto a Hybond-enhanced chemiluminescence nitrocellulose transfer membrane (Amersham Pharmacia) using a mini transblot system (Bio-Rad) in transfer buffer (25 mM Tris-HCl, 190 mM glycine, 20% methanol, pH 8.3). The membranes were soaked in PBS-T (20 mM Na_2HPO_4, 1.8 mM K_2HPO_4, 150 mM NaCl, 2.7 mM KCl, 0.1% Tween 20, pH 7.4) supplemented with 5% nonfat milk powder. This was followed by incubation with peroxidase-conjugated anti-His Ab 1/7000 (Sigma, St. Louis, MO, USA). The Ab was diluted in the blocking solution PBS-T milk 1%. Proteins on transferred membranes were revealed with tetramethyl-benzidine (TMB) (Sigma) after a wash with dextran sulfate 1% (Sigma).

Enzyme-linked immunoassay (ELISA), refolding, and size exclusion chromatography

Polystyrene immunoplates were coated with 50 μl of 5 μM R13-BSA conjugated peptide in 0.05 M bicarbonate-carbonate buffer (pH 9.6). BSA was used as control. Different amounts of scFvs were added to the wells and incubated at 37°C. Binding was measured from the absorbance at 450 nm after the addition of peroxidase-conjugated anti-His Ab, followed by TMB. Refolding of scFv using stepwise dialysis was performed as described in ref 13. The scFvs C5 and B7 were subjected to analytical size exclusion chromatography on a Superdex 200 HR10/30 column (Amersham Pharmacia) on a fast protein liquid chromatography (FPLC) system (Amersham Pharmacia) at 21°C in PBS calibrated with SIGMA gel filtration standard proteins. The flow rate was 0.5 ml/min and the absorbance of the effluent stream was monitored at 280 nm (14, 15).

Synthetic peptides

Peptides were prepared by the solid-phase method of Merrifield, as described by Müller et al. (16), with a semiautomatic multisynthesizer NPS 4000 (NeoMPS SA, Strasbourg, France). Both P013 (EDDDDDFGMGALF) and R13 (EEEDDDMGFGLFD) peptides were derived from the 13 carboxyl-terminal amino acids of the *T. cruzi* P0 (TcP0) and TcP2β protein, respectively. Peptides were coupled at a molar ratio of 1:30 to BSA with 0.05% glutaraldehyde as described in ref 16. The H26R peptide (HWWRAESDEARRCYNDPKCCDFVTNR) corresponds to amino acids 197–222 of the human β_1-AR (17).

Physicochemical characterization of the scFv fragment

A BIACORE 3000 instrument was used to determine the kinetic parameters of the different scFvs with either the recombinant proteins (TcP0 and TcP2β) or different peptides (R13 and H26R). All the reagents for analysis were obtained from BIACORE (Uppsala, Sweden). Three different conditions were used (**Fig. 1**). *A)* scFv as ligand. The scFvs C5 and B7 together with a control scFv were immobilized on a NTA chip. The chip was previously washed with EDTA and regenerated with a $NiCl_2$ solution at a flow rate of 10 μl/min for 1 min (as prescribed by the purveyors). Antigens were injected at a flow rate of 20 μl/min for 3 min, followed by a dissociation phase of 3 min. The NTA matrix was regenerated with EDTA solution. *B)* scFv as analyte. The low carboxylated dextran matrix (B1) was activated with 35 μl of a mixture 0.2 M *N*-ethyl-*N*-dimethylaminopropyl carbodiimide and 0.05 M *N*-hydroxysuccinimide at 5 μl/min. TcP2β-GST and TcP0-GST fusion proteins together with GST were immobilized with the standard BIACORE protocol at a density of 0.05 pmol/mm^2. The scFvs C5 and B7 were injected and kinetic studies were performed as described in ref 18. *C)* Inhibition. The scFv C5 was preincubated with different concentrations of either R13 or H26R peptides for 30 min, then injected on the sensor chip containing high density of TcP2β-GST fusion protein. Under this mass transfer condition, the slope of the curves is directly correlated with the active concentration of scFv (19). The IC_{50} (the concentration needed to inhibit 50% of the scFv-TcP2β interaction) was calculated from a logit plot (Sigmaplot). In all cases the sensorgrams were analyzed by global fitting using the Biaeval 1.4 program.

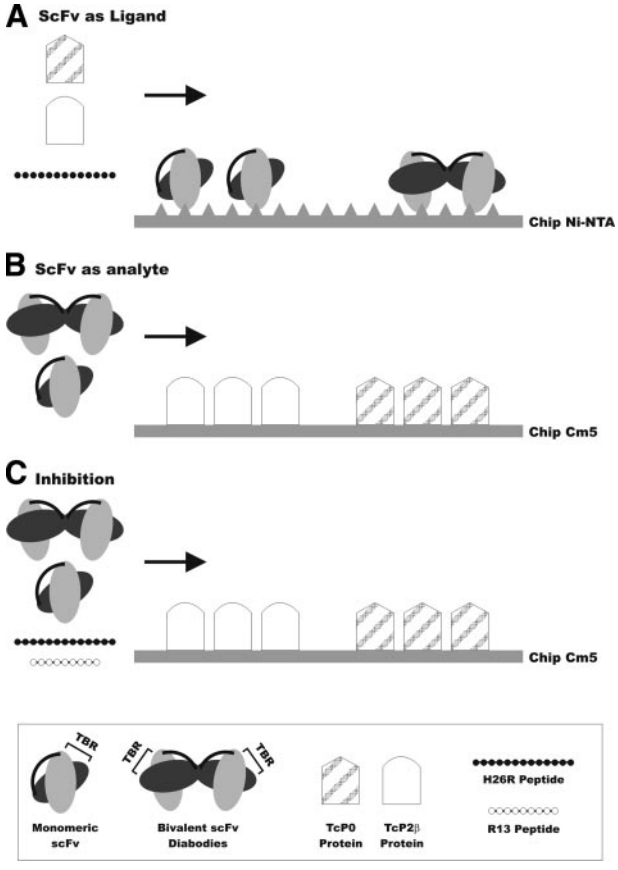

Figure 1. Schematic representation of BIACORE determinations. *A)* ScFv as ligand: the scFvs were fixed to a Ni-NTA chip and the recombinant proteins or the peptides flowed in solution. *B)* ScFv as analyte: the recombinant proteins were fixed to a CM5 chip and the scFvs flowed in solution. *C)* Inhibition: the recombinant proteins were fixed to a CM5 chip and scFv C5, preincubated with different concentration of peptides, flowed in solution. TBR: target binding region.

Immunocytochemistry

Stably transfected CHO-K cells expressing the human β_1-AR and nontransfected cells were washed twice with ice-cold PBS, pH 7.4, and fixed with 3.8% (v/v) of formaldehyde/PBS. The residual formaldehyde was quenched by addition of 0.02 M glycine in PBS, pH 7.4. After blocking with PBS-BSA 5%, the cells were incubated with mAb anti-β_1 (150 nM), mAb 17.2 (300 nM), or scFvs (200 nM). Their binding to CHO-K cells was detected using FITC-labeled goat antimouse IgG (H+L) (Jackson ImmunoResearch, Baltimore, MD, USA) for mAbs and with mouse anti-His tag (Invitrogen, Carlsbad, CA, USA), followed by a FITC-labeled goat antimouse IgG for scFvs. Competition experiments were performed by preincubation of mAbs or scFvs with either H26R peptide (1 μM) or R13 peptide (100 nM) for 1 h at room temperature. Cells were visualized using a Zeiss confocal microscope LSM-510 system with a highly corrected objective (C-Apochromat ×40 numerical aperture 1.2 underwater). The same conditions were used for fixed parasites. Images were processed using Image Browser 3.0 and Photoshop 6.0.

Bystander activation of the β_1-AR

The biochemical effects of the scFvs C5 and B7 on β_1-AR recognition were assessed by measuring total cAMP levels on CHO-K β_1-AR transfected cells (6). Cells were seeded onto 96-well culture plates 24 h before stimulation, washed with PBS, and incubated with 1 ml of Hanks' balanced medium buffered with 10 mM HEPES plus 100 μM isobutylmethylxanthine (cAMP hydrolysis blocker). Thereafter, cells were incubated with different concentrations of the scFvs, 1 h at 37°C, while isoproterenol (ISO) (Sigma) was added for 5 min at 37°C. The cAMP concentration was determined using a competitive immunoenzymatic assay (BIOTRAK cAMP, Amersham Pharmacia). Competition experiments were performed by preincubation of mAbs or scFvs with either H26R peptide (250 nM) or R13 peptide (250 nM) for 1 h at room temperature. Results were expressed as % increase of cAMP concentrations over basal values. The basal cAMP levels correspond to cells treated with PBS under the same conditions. Results were from duplicates of three independent experiments and were compared by Student's *t* test. Statistical analysis was performed using Graphpad software.

Measurement of beating frequency of neonatal rat cardiomyocytes

Rat neonatal cardiomyocytes were prepared from hearts of 1- to 2-day-old Sprague Dawley rats as described (4, 5). The cells

were cultured as monolayers for 4 days at 37°C in Dulbecco's modified Eagle medium-F12 medium supplemented with 10% heat-inactivated calf serum and 0.1% glucose, and exhibited a spontaneous basal pulsation rate of ~160 beats/min. The cardiomyocyte cultures were washed with fresh medium without serum and incubated for 60 min at 37°C. Single beating cells or clusters of synchronously beating cardiomyocytes in each of the 10 fields were selected, and the number of contractions counted for 15 s. This procedure was repeated for two to five identically treated culture flasks. scFvs were incubated with the monolayer for 60 min.

Physiological characterization of the scFv fragment *in vivo*

Mice were maintained in accordance with the Guide for the care and use of laboratory animals (National Research Council, National Academic Press, Washington, DC, 1996). Five female BALB/c mice, 20 g each, were used for each condition using Tribromoethanol 150 mg/kg intraperitoneal as anesthetic. Five different conditions were assessed: *1)* mice intravenously (i.v.) injected with 200 μl of either scFv C5 or scFv B7, 250 nM; *2)* mice i.v. injected with 200 μl of either scFv C5 or scFv B7, 500 nM; *3)* mice i.v. injected with 2 mg/kg body wt of ISO; *4)* mice i.v. injected with 200 μl of either scFv C5 or scFv B7, 250 nm, followed after 5 min by injection of ISO; *5)* mice i.v. injected with 200 μl of either scFv C5 or scFv B7, 500 nM, followed after 5 min by an injection of ISO. Electrocardiogram (ECG) recordings were performed during 20 min after injection. ECGs were obtained with the six standard leads (I, II, III, AVR, AVL, AVF) at 50 mm/s of paper speed and at 20 mm/mV amplitude using a Fukuda-Denshi Fx-2111 electrocardiograph (Tokyo, Japan) (8,9). Electrocardiographic analysis included measurements of heart rate, P wave duration, and amplitude, QRS complex duration and amplitude, P-R interval duration and a search for disturbances of rhythm, conduction, and repolarization. The cardiac rhythms of scFv-treated mice and mice injected with PBS (control mice) were compared by Student's *t* test. Statistical analysis was performed using Graphpad software.

Molecular modeling

All procedures were performed with Insight II, Biopolymer, Homology, Docking and Discover software from Accelrys (San Diego, CA, USA). The high similarity of the combining sites of mAb 17.2 with that of a known 3-dimensional structure (PDB 1NBV) (20), corresponding to an Ab against DNA, allowed us to construct a realistic model of the Ab combining site *in silico*. We proceeded to manually change the amino acids that were different from the 1NBV sequence (20). We minimized the obtained structure until the RMS deviation was < 0.001 Kcal/mol by conjugated gradient under distant dependent dielectric constant after charging the Ab combining site at pH = 7.4 and fixing the backbone with the exception of the CDR regions.

To identify the critical residues of the antigen-combining site, two decapeptides were docked into the structural model: the epitopic target of the TcP2β protein HCO-EDDDMGF-GLF-NH_2 and the epitopic target of the second extracellular loop of the β_1-AR HCO-ESDEARRCYN-NH_2. Docking of both peptides was performed manually using the charged peptide structure, which was minimized under conditions of a dielectric constant of 80. A negative intermolecular energy (being the sum of Vander Waals and Coulombic forces) was obtained before the complex was minimized by a conjugate gradient in a distant dependent dielectric constant. The obtained structure was further submitted to a dynamic simulation at 300°K of 110 ps (10 ps equilibrium and 100 ps dynamics) fixing the framework amino acids, and allowing the CDR regions and the peptide to move. A conformation with lower potential energy was obtained. This conformation was again subjected to conjugate gradient minimization.

RESULTS

Expression of four scFv fragments derived from mAb 17.2

Active immunization with the recombinant TcP2β protein established the protocol that was used to generate mAb 17.2. This mAb reacts with the C-terminal R13 epitope of TcP2β and has β_1-AR-stimulating properties (10). Messenger RNA obtained from hybridoma cell cultures was used to amplify the variable regions of the mAb 17.2 that were assembled as four different scFvs. Each construction differed in the length of the linker and/or the order of the variable regions. ScFvs C5 and B7 have the same arrangement of variable regions, namely VH-VL, but they are linked either by a short linker sequence encoding for five amino acids or by a long one encoding for 15, respectively. ScFvs F4 and G12 have a VL-VH arrangement, but the former included the short linker and the latter the longer one (**Fig. 2*A***). Recombinant Abs were purified from the periplasmic space of HB2151 *E. coli* cells and concentrated by Nickel affinity chromatography using the 6×His (Fig. 2*B*). The four scFvs were tested for their reactivity against either R13 peptide or recombinant TcP2β protein by ELISA (Fig. 2*C*, left and data not shown). The reactivity of scFv F4 was only evident after refolding (Fig. 2*C*, right) and led us to exclude this scFv from further analysis. Since the length of the linker determines the oligomeric status of a scFv, the scFvs C5 and B7 were analyzed by size exclusion chromatography (15). The purified scFv C5 ran as a dimmer showing a peak that corresponds to ~55 kDa, whereas the purified scFv B7 ran as a monomer with a size of ~30 kDa (Fig. 2*D*).

The VH and VL domains of the scFvs were sequenced and the nucleotide (nt) sequences were compared with those of known germline genes. The VH region showed 98% identity to the mouse H-chain germline gene MRL-DNA4 (PMID M21470) (**Fig. 3*A***). The VL region shared 98% homology with the mouse L-chain germline gene bd2 (PMID AJ231196) (Fig. 3*B*).

Immunochemical characterization of mAb 17.2-derived scFvs

The mAb 17.2 was able to recognize the C-terminal end of all five *T. cruzi* ribosomal P proteins (**Fig. 4*A***, right). This was due to the fact that four of them contain the R13 epitope, TcP1 α, TcP1 β, TcP2α, and TcP2β; the fifth, TcP0, has a slightly different but highly acidic C-terminal epitope homologous to R13 (8, 21). As was the case for the monoclonal, all three scFvs (C5, B7, and G12) recognized the recombinant TcP2β protein

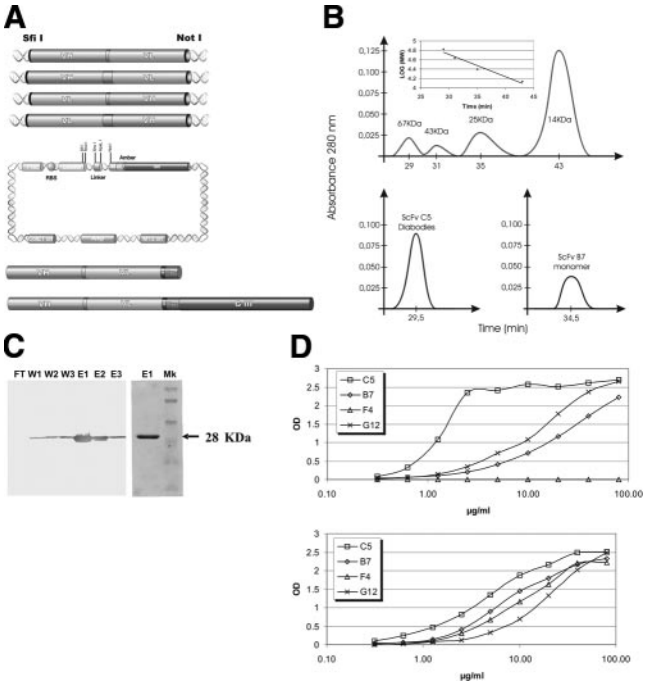

Figure 2. Activity and oligomerization properties of purified scFvs. *A)* Schematic representation of the expression cassettes for mAb 17.2-derived constructs. The pHen II vector: locations of ribosome binding site (RBS), pelB leader sequence (Leader), multiple cloning site, six-histidine tag (HIS), c-*myc* epitope (MIC), and the amber stop codon (Amber) are indicated. Differential production of fusion proteins depending on the host *E. coli* strain is also represented. *B)* Nickel affinity purification of a periplasmic extract (scFv C5). The flow-through (FT), wash (Wn), and elution (En) of the purified scFv are indicated. On the right, Coomassie staining of eluted fraction 1. *C)* ELISA reactivity to the R13 peptide of the four purified scFv constructs. Left panel: binding of purified scFvs. Right panel: binding of refolded scFvs. *D)* Size exclusion chromatography of the purified scFvs C5 and B7 on a calibrated Superdex 200 gel filtration column. Elution time of protein markers: 67 kDa, BSA; 43 kDa, ovalbumin; 25 kDa, chymotrypsinogen; 14 kDa, ribonuclease A. Linear regression of log (MW) vs. elution time with a R^2 of 0.962 (inset). Elution times for scFvs C5 and B7 are indicated.

(data not shown). They also recognized the five ribosomal P proteins in Western blot of purified *T. cruzi* ribosomes, as exemplified for C5 (Fig. 4*A*, left). MAb 17.2 and its derived scFvs also reacted with fixed parasites, where they exhibit a granular cytoplasmic recognition pattern (Fig. 4*B*).

Surface plasmon resonance was used to characterize and compare the binding of the different Abs to the *T. cruzi* ribosomal P proteins and to R13 and H26R peptides. Direct binding of mAb 17.2 to TcP2β showed an affinity constant of 3 nM, and its Ki for R13 was 400 nM (10). ScFv C5 showed a similar binding affinity to TcP2β (K_d=8 nM) whereas the scFv expression product with a long linker, B7, had less affinity (K_d=46 nM) under conditions in which scFvs were used as ligands (Fig. 1*A*, **Table 1** and **Fig. 5*A***). In contrast, when scFv C5 was used as analyte on immobilized TcP2β or TcP0 proteins, the apparent affinities were 0.2 nM and 11 nM, respectively (Fig. 1*B*, Table 1, and Fig. 5*B*). These results stress the importance of avidity. Using the same conditions for scFv B7, affinity constants were 20 nM for TcP2β protein, suggesting reduced avidity, and thus monovalent binding.

Although mAb 17.2 had a β_1-AR-stimulating effect, we were not able to measure its binding to the H26R peptide. Using the scFv C5 as ligand, the affinity constant representing the binding of scFv C5 to H26R was 10 μM (Table 1 and Fig. 5*A*). The specificity of this binding was confirmed in experiments in which the H26R peptide was used to inhibit the binding of scFv C5 to TcP2β. An IC_{50} of 12 μM was obtained, confirming the affinity of the direct binding experiment (Fig. 1*C*, Table 1, and Fig. 5*C* right). The R13 peptide inhibited the binding of the scFv C5 to TcP2β with an IC_{50} of 725 nM (Table 1 and Fig. 5*C*, left). Unrelated peptides of approximately the same size had no effect on scFv C5-TcP2β interaction (data not shown).

The ability of mAb 17.2 and both scFvs C5 and B7 to bind to the β_1-AR was also determined by immunocytochemistry of CHO-K cells stably transfected with the receptor. ScFvs C5 and B7 reacted with the transfected cells, where they display specific membrane and cyto-

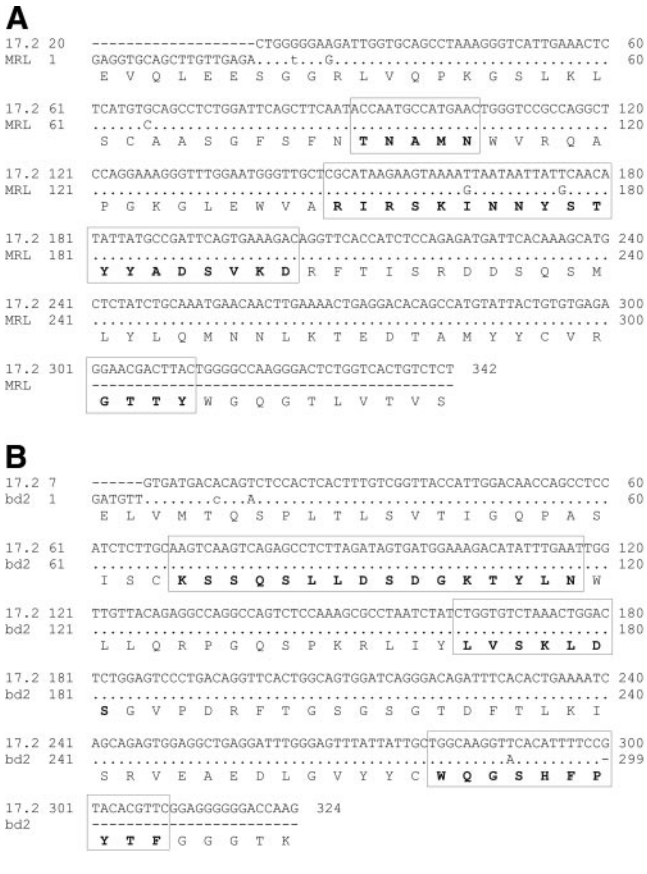

Figure 3. Sequence of the heavy (*A*) and light (*B*) chain variable regions of mAb 17.2. The nt sequence of the variable regions of mAb 17.2 were compared with the closest germline genes. Identities are indicated by dots. Capital and lowercase letters indicate replacement and silent mutations, respectively. The deduced amino acid sequences of the rearranged heavy and light chains of the mAb 17.2 are also shown. The complementary determining regions (CDRs) are boxed.

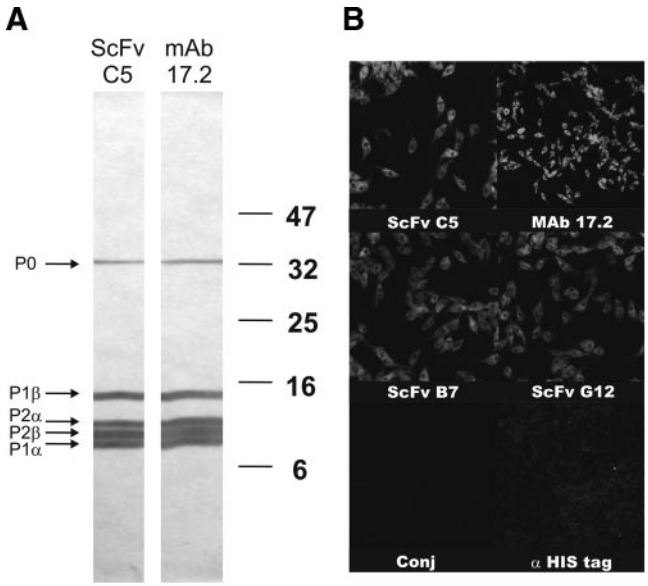

Figure 4. Reactivity of the scFvs against *T. cruzi* ribosomal P proteins. *A)* Reactivity of the scFv C5 and mAb 17.2 against purified *T. cruzi* ribosomes. The five ribosomal P proteins are indicated. *B)* Immunocytochemistry on fixed *T. cruzi* cells with different scFvs and mAb 17.2.

plasmic labeling. The interactions of both scFvs to CHO-K cells were blocked by the addition of excess of R13 and H26R peptides (**Fig. 6*A***). Control experiments, utilizing either transfected cells in the absence of scFv or nontransfected cells with scFv, revealed a very low concentration of background staining, confirming the specificity of mAb 17.2, scFv C5, and scFv B7 binding to the receptor.

Bystander activation of the β_1-AR

CHO-K cells stably expressing β1-AR were also used to determine the pharmacological properties of both scFvs C5 and B7 and compare them to those of mAb 17.2. Activation of the β_1-AR was monitored as a change in total cAMP concentration (Fig. 6*B*). ScFv C5 stimulated the β_1-AR in a concentration-dependent manner. On the other hand, scFv B7 had no apparent effect on the β_1-AR, but inhibited ISO induced activation of the receptor in a dose-dependent manner, indicating that this scFv bound the receptor without activating it (Fig. 6*B*). These results were confirmed *in vitro* by assessing the effects of the recombinant Abs on the beating frequency of neonatal rat cardiomyocyte cultures. As shown in **Fig. 7*A***, scFv C5 induced a dose-dependent positive chronotropic effect. This effect decreased after treatment with the β-blocker propranolol, indicating a specific β_1-AR stimulation activity. ScFv B7 alone induced no chronotropic effect, but when added before ISO it blocked ISO's positive chronotropic effect. This occurred in a dose-dependent manner (data not shown), with a maximal effect at 250 nM (Fig. 7*B*). Altogether these results indicate that scFv C5, as a dimmer, has the ability to activate the receptor, whereas the monomer scFv B7 acts as a blocker. Both recombinant Abs exert their effects by direct recognition of the β_1-AR.

Physiological characterization of the scFv fragments

The *in vivo* effects of mAb 17.2, scFv C5, and scFv B7 were studied by passive transfer to naive mice, injecting i.v. either the Ab or the Ab fragments with or without ISO. The injection of mAb 17.2 induced a significant increase in heart beating rate, an effect that was maximal at 200 nM after 30 min of injection (data not shown). scFv C5 on its own also induced a significant increase in heart rate in a dose-dependent manner, with a maximal effect at 250 nM. Repolarization abnormalities (**Fig. 8*A***-a) and first degree AV conduction block (Fig. 8*A*-b) were recorded 5 min after injection and maintained for 10 min. Thereafter, basal beating frequency was slowly recovered. The injection of ISO (2 mg/kg) alone induced a marked increase in heart rate, whereas scFv B7 alone did not induce tachycardia but blocked, in a dose-response manner, the effect of ISO (Fig. 8*B*). This effect was observed only when scFv B7 was added before the ISO; when scFv B7 was added after ISO or simultaneously, it had no effect.

3-Dimensional model of the antigen combining site

The existence of a 3-dimensional structure of an Ab fragment (PDB 1NBV) with close similarity to the heavy and light chain of the mAb 17.2 allowed us to construct a 3-dimensional model of the mAb 17.2 combining site that interacts with either TcP2β or β_1-AR-derived pep-

TABLE 1. *Kinetic parameters*[a]

		Ligand	Analyte	Inhibition
	TcP2β	K_d = 8 nM	K_d = 0,2 nM	ND
	TcP0	K_d = 38 nM	K_d = 11 nM	ND
	H26R	K_d = 10 μM	ND	IC_{50} = 12 μM
scFv C5	R13	NM	ND	IC_{50} = 725 nM
scFv B7	TcP2β	K_d = 46 nM	K_d = 20 nM	ND

[a] Kinetic parameters determined for the different scFvs against the recombinant proteins TcP2β and TcP0, and the H26R peptide. Kds were determined from the association and dissociation rate constants using a Langmuir binding model. The IC_{50} for both R13 and H26R peptides was calculated from a logit plot. ND, not determined; NM: not measurable.

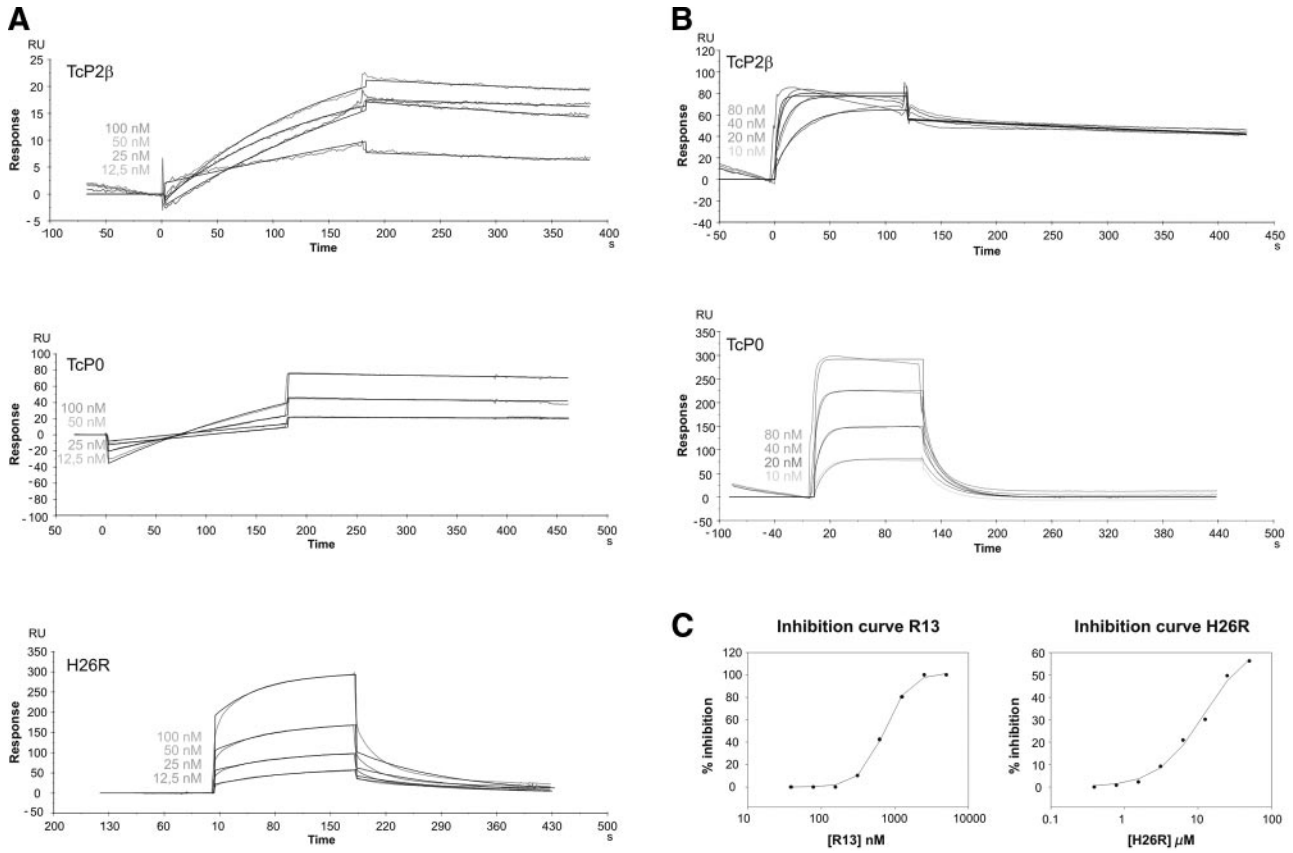

Figure 5. Biacore sensograms of scFv C5. *A)* Interaction of scFv C5 with recombinant proteins TcP2β and TcP0 and with the H26R peptide (scFv as ligand, Fig. 1*A*). *B)* Interaction of scFv C5 with the recombinant proteins TcP2β and TcP0 (scFv as analyte, Fig. 1*B*). *C)* Inhibition of scFv C5-TcP2β interactions with R13 (left) and H26R (right) peptides (Fig. 1*C*).

tides (**Fig. 9*A***). The template used for modeling corresponds to an anti-DNA Ab crystallized at level 2Å resolution (20). At the amino acid level, both VH and VL of PDB 1NBV fragments share 86% and 71% identity with the VH and VL chains of mAb 17.2, respectively. This allowed us to construct a realistic model of its antigen combining site *in silico*. Figure 9*B*, shows that 9 of the 10 amino acids of the TcP2β peptide, EDDDMGFGLF, are predicted to interact with 25 CDR residues, forming two salt bridges (Glu1–ArgH52 and Asp4– LysL58) and 9 hydrogen bonds. In comparison, 9 of the 10 residues of the β_1-AR peptide, ESDEARRCYN, are predicted to interact with 21 CDR residues forming 3 salt bridges (Glu1-ArgH52, Glu1-ArgH50 and Glu4-LysL58) and 12 hydrogen bonds (Fig. 9*C*). Moreover, Phe8 of the TcP2β peptide is surrounded by four hydrophobic residues (TyrL37, LeuL55, TrpL94 and TyrL101) while Tyr9 in the β1-AR peptide is surrounded by three aromatic residues (TyrL37, PheL99, TyrL101). These differences are mainly responsible for the calculated lower intermolecular energy (–965 Kcal/mol) of the TcP2β peptide-scFv complex compared to that of the β_1-AR peptide (–504 Kcal/mol). The model estimates that the number of contact residues, i.e., the number of residues that have at least one atom 3Å distance from each epitope residue on the paratope (12 of the VH and 15 of the VL for the interaction with the TcP2β peptide, and 11 of the VH and 12 of the VL for the β_1-AR peptide) is similar. Notably, the model predicts that 20 of the residues that contact the parasite peptide would also contact the peptide of the β_1-AR, explaining the cross-reactive nature of the mAb 17.2 and its derived recombinants. This model may also explain the cross-reaction of mAb 17.2 with rhodopsin (22).

DISCUSSION

Although several studies have proposed that parasite-derived proteins might induce Abs with the ability to react with self-structures causing tissue damage and/or alteration of normal physiological function, only partial evidence to support these claims has been presented (23–27). This study was designed to unambiguously prove that an Ab raised against the C-terminal end of the parasite ribosomal P protein is able to stimulate a cardiac receptor and to define the most accurate model possible to depict the residues involved in this parasite-self cross-reaction.

Previous studies demonstrated that immunization with the ribosomal TcP2β protein induced an arrythmogenic response that was strictly associated with an increased concentration of Abs against the C-terminal end of the parasite protein, the R13 epitope (8, 9, 28). These initial immunization protocols led to the production of the anti-R13 mAb, named 17.2 (10, 29). Results

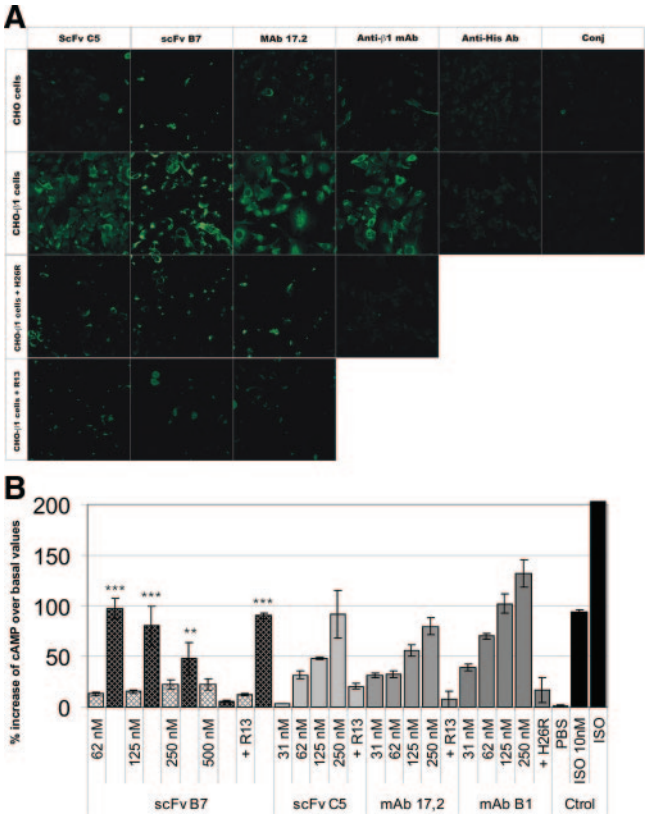

Figure 6. Recognition and activation of human β_1-AR on CHO-K cells. *A)* Immunocytochemical determination of Ab binding to CHO-K cells stably transfected with the human β_1-AR. The reactivities of both scFvs C5 and B7 were compared with those of mAb 17.2 and mAb anti-β_1. The binding of the Abs to the receptor was inhibited by preincubation of either H26R or R13 peptides (see Materials and Methods). *B)* Increase of cAMP levels of human β_1-AR stably transfected CHO-K cells incubated with different concentrations of scFv C5, scFv B7, and control mAbs. In scFv B7 assays, light shaded bars: addition of scFv alone; dark shaded bars: addition of scFv and 10 nM ISO; *results statistically different from those obtained with scFv alone, $P < 0.05$ in Student's t test.

in Fig. 4*A, B* showed that the mAb 17.2 reacted with the parasite ribosomal P proteins and demonstrated the cytoplasmic distribution of these proteins within the parasite. It also recognized the human β_1-AR, as shown by surface staining of CHO-K transfected cells (Fig. 6*A*). Consequently, passive transfer of mAb 17.2 induced supraventricular tachycardia in recipient animals (data not shown). However, mAb 17.2 failed to bind the peptide representing the second extracellular loop of the receptor in all experimental settings, including surface plasmon resonance.

Four recombinant Abs were derived from mAb 17.2. Two of them, with the VH-VL configurations representing variations of the original Ab, had quite contrasting properties. ScFv C5 had a higher affinity to TcP2β than mAb 17.2, whereas scFv B7 had a lower affinity for the ribosomal protein (Table 1). scFv C5 also had higher affinity to TcP0 than mAb 17.2, indicating that the arrangement of variable regions and the short linker generated an Ab with higher affinity for substrates recognized by mAb 17.2 (Table 1). Functional assays demonstrated that this Ab displayed a β_1-AR-stimulating activity. Notably, using surface plasmon resonance only scFv C5 had a measurable affinity for the β_1-AR-derived H26R peptide, in either direct binding studies or indirect inhibition assays (Table 1, Fig. 5*A, C*). To our knowledge, these measurements are the first to document unambiguously that an Ab induced by a *T. cruzi* intracellular protein has the ability to react with a human peptide representing an essential extracellular domain of a cardiac receptor.

The apparent higher affinity of scFv C5 is likely to be a consequence of the arrangement of mAb 17.2 variable regions and the 5 amino acid-long sequence that links them generating a diabody. Indeed, the monovalent version of this recombinant had a 15 amino acid linker and bound TcP2β with less affinity (Table 1), but had no measurable binding to the H26R peptide. Although both mAb 17.2 and scFv C5 are bivalent, it is tempting to speculate that the spatial geometry of the binding sites of the recombinant Ab increase its avidity for the different epitopes. Like mAb 17.2, scFv C5 also has a β_1-AR-stimulating effect both *in vitro* and *in vivo* (Figs. 7, 8). In contrast, acting as a monomer, scFv B7 blocks the effect of ISO both *in vitro* and *in vivo* (Figs. 7, 8). More generally, these results support the notion that Abs against cardiac receptors, not only those described in Chagas disease (6), exert their effects by favoring receptor dimerization and consequently receptor activation. The monovalent scFv B7 blocked the

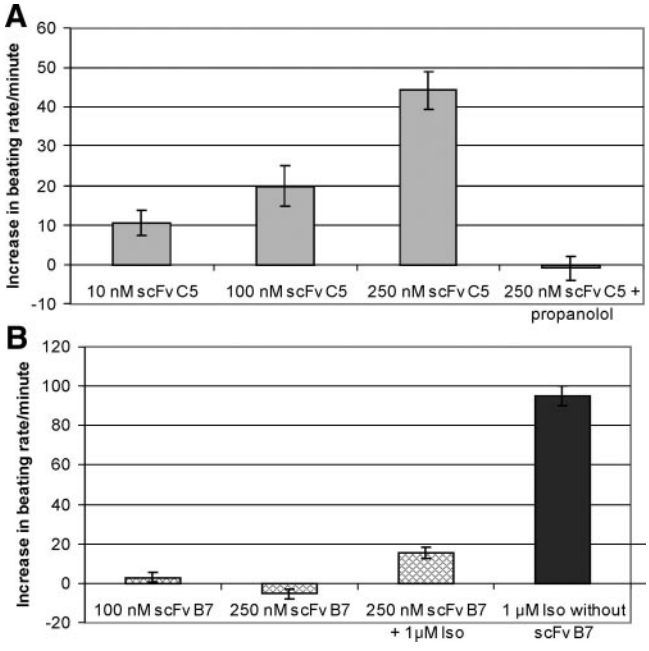

Figure 7. Chronotropic effect of scFvs C5 and B7 on neonatal rat cardiomyocytes. *A)* Dose-dependent response produced by incubation of cardiomyocytes with increasing amounts of scFv C5 and reversion of the effect with the β-blocker propranolol 1 μM. *B)* svFv B7 inhibition of the response to ISO (1 μM) in a dose-dependent manner. The effects were determined as an increase in beating frequency/min. The abscissa shows the different conditions under which the activity was measured.

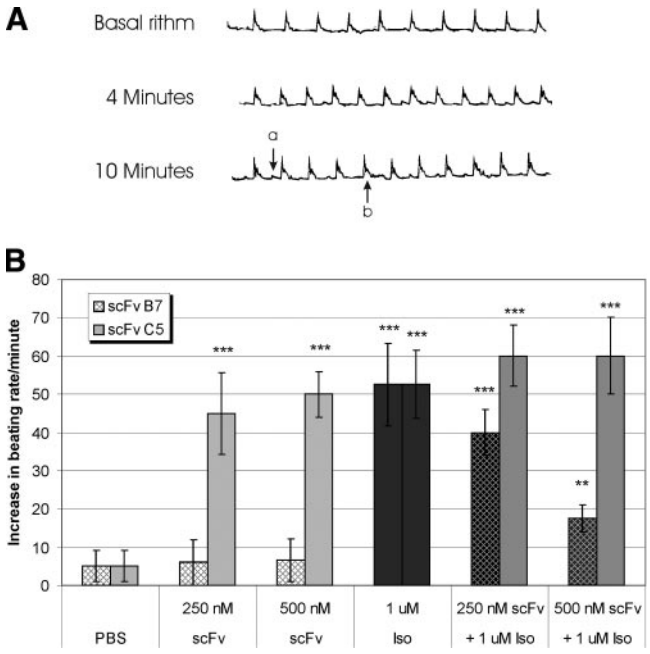

Figure 8. Passive transfer of scFvs C5 and B7 to mice. *A)* ECG tracings of BALB/c mice treated with 200 μl of scFv C5 250 nM i.v. Recordings before injection, 4 and 10 min after injection are shown. The abnormalities observed are indicated (a, b) and discussed in the corresponding section. *B)* Mean of the variation of cardiac rhythm 10 min after i.v. injection of either scFv C5 or B7, with or without ISO (2 mg/kg). *Results statistically different from experiments without scFv (PBS); $P < 0.05$ in Student's t test.

agonist activation probably by closing the pharmacophoric pocket, as already described for recombinant Abs against the β_2-adrenergic and the M_2 cholinergic receptors (30, 31). This is also in line with the importance of the second extracellular loop of G-protein coupled receptors (GPCRs) in locking receptor activity (32).

Docking of the R13 peptide within the modeled structure of the mAb 17.2 revealed how the binding pocket of the Ab may recognize the residues involved in R13 antigenicity, Glu 3, and Asp 6 (7–9). This model also explains the reactivity of anti-R13 Ab with the acidic residues of the second extracellular loop of the β_1-AR. Considering the pentapeptide AESDE of H26R peptide, the second and fifth Glu residues (xExxE) are arranged in a manner that resembles that of Glu 3 and Asp 6 in R13 (xExxD). Patients with anti-R13 Abs with β_1-AR-stimulating properties also recognize noncontiguous acidic residues of the R13 peptide (7).

The results described here constitute a clear demonstration that Abs raised against the C-terminal end of the *T. cruzi* ribosomal P proteins can cross-react with the second extracellular loop of the human β_1-adrenergic receptor, causing its stimulation. Because high levels of anti-R13 Abs have been detected in severe cases of the disease (4–7, 33–35), it is tempting to hypothesize that at high blood concentrations the agonist-like properties of these Abs may exert a wider effect by inducing functional changes in cell types and tissues expressing this receptor or related GPCRs, such as rhodopsin (22), thereby increasing the liability of a chronic infected organism. FJ

The authors gratefully acknowledge S. Ansaldi (Ramos Mejia Hospital, Buenos Aires, Argentina) for constant advice, counseling, and interpretation of mice electrocardiograms; undergraduate student L. Simonetti for preparation of recombinant antibodies used in the later stages of experiments; Dr. G. Alonso (INGEBI) for assistance in FPLC experiments; and Dr. G. Langsley (Inst. Cochin, Paris, France) for correcting English. The authors also acknowledge Dr. R. Mobini for kindly sending and allowing the use of mAb anti-β_1-AR in these studies (Wallenberg Laboratory for Cardiovascular Research, Goteborg, Sweden). During the entire development of this work, M.J.L. was mainly supported by an International Research Grant of Howard Hughes Medical Institute (Chevy Chase, MD, USA). This research was also supported by grants from the World Health Organization/Special Program for Research and Training in Tropical Diseases; Universidad de

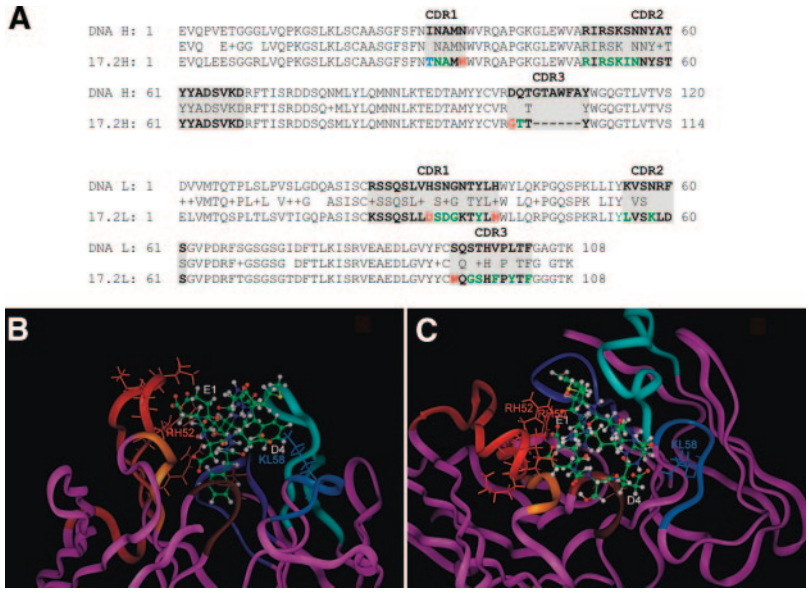

Figure 9. Model of the scFv combining site. *A)* The amino acid sequence of the mAb 17.2, heavy and light chains (17.2H and 17.2L, respectively) were compared with the structure templates used for molecular modeling (PDB 1NBV), named DNA. The CDRs are in boldface. The modeled contact residues of mAb 17.2 specific for the TcP2β-derived peptide are in red, those specific for the β_1-AR-derived peptide are in blue, and those contacting the two peptides are in green. *B)* Model of the Ab interaction with the TcP2β-derived peptide. CDR L1 is in light blue, L2 in blue, L3 in dark blue, H1 in orange, H2 in red, and H3 in brown. The amino acids involved in electrostatic interactions with peptide residues E1 and D4 are represented as sticks. The TcP2β-derived peptide (CHO-E-D-D-D-M-G-F-G-L-F-NH_2) is represented in stick and balls. *C)* Model of the Ab interaction with the β_1-AR-derived peptide (CHO-E-S-D-E-A-R-R-C-Y-N) represented in stick and balls. The amino acids involved in electrostatic interactions with the peptide residues E1 and E4 are represented as sticks.

Buenos Aires, Ministerio de Salud y Acción Social-Beca Ramón Carrillo-Arturo Oñativia, and the National Agency of Scientific and Technological Promotion (FONCYT BID 1201/OC-AR 01–14389). Support of CNRS-CONICET (2001–2002) and INSERM-CONICET (2002–2003) collaborative French-Argentinean research grants, as well as the ECOS-Sud project "Anticorps antiproteines ribosomales P de *T. cruzi* comme inhibiteur specifique de la traduction" (France-Argentine, 2005–2008) is acknowledged. This article was written as M.J.L. was international professor (2005–2006) of a Chaire Internationale de Recherche Blaise Pascal, Fondation Ecole Normale Superieure, Region Ile de France, Paris, France.

REFERENCES

1. Elizari, M. V., and Chiale, P. A. (1993) Cardiac arrhythmias in Chagas' heart disease. *J. Cardiovasc. Electrophysiol.* **4,** 596–608
2. Halperin, C., and Rassi, S. (2000) Clinical relevance of invasive electrophysiologic studies in patients with Chagas' disease. In *Arrhythmia Management in Chagas' Disease,* pp. 83–93, Futura Publishing Co. Inc., Armonk, NY
3. Rosenbaum, M. B., Chiale, P. A., Schejtman, D., Levin, M., and Elizari, M. V. (1994) Antibodies to beta-adrenergic receptors disclosing agonist-like properties in idiopathic dilated cardiomyopathy and Chagas' heart disease. *J. Cardiovasc. Electrophysiol.* **5,** 367–75
4. Elies, R., Ferrari, I., Wallukat, G., Lebesgue, D., Chiale, P., Elizari, M., Rosenbaum, M., Hoebeke, J., and Levin, M. (1996) Structural and functional analysis of the B cell epitopes recognized by anti-receptor autoantibodies in patients with Chagas' disease. *J. Immunol.* **157,** 4203–4211
5. Kaplan, D., Ferrari, I., Bergami, P. L., Mahler, E., Levitus, G., Chiale, P., Hoebeke, J., Van Regenmortel, M. H., and Levin, M. J. (1997) Antibodies to ribosomal P proteins of *Trypanosoma cruzi* in Chagas disease possess functional autoreactivity with heart tissue and differ from anti-P autoantibodies in lupus. *Proc. Natl. Acad. Sci. U.S.A.* **16,** 10301–10306
6. Chiale, P. A., Ferrari, I., Mahler, E., Vallazza, M. A., Elizari, M. V., Rosenbaum, M. B., and Levin, M. J. (2001) Differential profile and biochemical effects of antiautonomic membrane receptor antibodies in ventricular arrhythmias and sinus node dysfunction. *Circulation* **103,** 1765–1771
7. Mahler, E., Hoebeke, J., and Levin, M. (2004) Structural and functional complexity of the humoral response against the *Trypanosoma cruzi* ribosomal P2β protein in patients with chronic Chagas' heart disease. *Clin. Exp. Immunol.* **136,** 527–534
8. Lopez-Bergami, P., Scaglione, J., and Levin, M. J. (2001) Antibodies against the carboxyl-terminal end of the *Trypanosoma cruzi* ribosomal P proteins are pathogenic. *FASEB J.* **15,** 2602–2612
9. Lopez Bergami, P., Gomez, K. A., Levy, G. V., Grippo, V., Baldi, A., and Levin, M. J. (2005) The β1 adrenergic effects of antibodies against the C-terminal end of the ribosomal P2β protein of *Trypanosoma cruzi* associate with a specific pattern of epitope recognition. *Clin. Exp. Immunol.* **142,** 140–147
10. Mahler, E., Sepulveda, P., Jeannequin, O., Liegeard, P., Gounon, P., Wallukat, G., Eftekhari, P., Levin, M. J., Hoebeke, J., and Hontebeyrie, M. (2001) A monoclonal antibody against the immunodominant epitope of the ribosomal P2β protein of *Trypanosoma cruzi* interacts with the human β1-adrenergic receptor. *Eur. J. Immunol.* **31,** 2210–2216
11. Griffiths, A. D., Williams, S. C., Hartley, O., Tomlinson, I. M., Waterhouse, P., Crosby, W. L., Kontermann, R. E., Jones, P. T., Low, N. M., Allison, T. J., et al. (1994) Isolation of high affinity human antibodies directly from large synthetic repertoires. *EMBO J.* **13,** 3245–3260
12. Mousli, M., Devaux, C., Rochat, H., Goyffon, M., and Billiald, P. (1999) A recombinant single-chain antibody fragment that neutralizes toxin II from the venom of the scorpion Androctonus australis hector. *FEBS Lett.* **15,** 183–188
13. Asano, R., Kudo, T., Nishimura, Y., Makabe, K., Hayashi, H., Suzuki, M., Tsumoto, K., and Kumagai, I. (2002) Efficient construction of a diabody using a refolding system: anti-carcinoembryonic antigen recombinant antibody fragment. *J. Biochem.* **132,** 903–909
14. Kortt, A.A., Malby, R. L., Caldwell, J. B., Gruen, L. C., Ivancic, N., Lawrence, M. C., Howlett, G. J., Webster, R. G., Hudson, P. J., and Colman, P. M. (1994) Recombinant anti-sialidase single-chain variable fragment antibody. Characterization, formation of dimer and higher-molecular-mass multimers and the solution of the crystal structure of the single-chain variable fragment/sialidase complex. *Eur. J. Biochem.* **1,** 151–157
15. Kortt, A.A., Lah, M., Oddie, G. W., Gruen, C. L., Burns, J. E., Pearce, L. A., Atwell, J. L., McCoy, A. J., Howlett, G. J., Metzger, D. W., Webster, R. G., and Hudson, P. J. (1997) Single-chain Fv fragments of anti-neuraminidase antibody NC10 containing five- and ten-residue linkers form dimers and with zero-residue linker a trimer. *Protein Eng.* **10,** 423–433
16. Muller, S., Couppez, M., Briand, J. P., Gordon, J., Sautie′re, P., and Van Regenmortel, M. H. V. (1985) Antigenic structure of histone H2B. *Biochim. Biophys. Acta* **827,** 235–246
17. Frielle, T., Collins, S., Daniel, K. W., Caron, M. G., Lefkowitz, R. J., and Kobilka, B. K. (1987) Cloning of the cDNA for the human β1-adrenergic receptor. *Proc. Natl. Acad. Sci. U.S.A.* **84,** 7920–7924
18. Mijares, A., Lebesgue, D., Wallukat, G., and Hoebeke, J. (2000) From agonist to antagonist: Fab fragments of an agonist-like monoclonal anti-beta(2)-adrenoceptor antibody behave as antagonists. *Mol. Pharmacol.* **58,** 373–379
19. Richalet-Secordel, P. M., Rauffer-Bruyere, N., Christensen, L. L., Ofenloch-Haehnle, B., Seidel, C., and Van Regenmortel, M. H. (1997) Concentration measurement of unpurified proteins using biosensor technology under conditions of partial mass transport limitation. *Anal. Biochem.* **249,** 165–173
20. Herron, J. N., He, X. M., Ballard, D. W., Blier, P. R., Pace, P. E., Bothwell, A. L., Voss, E. W., Jr., and Edmundson, A. B. (1991) An autoantibody to single-stranded DNA: comparison of the three-dimensional structures of the unliganded Fab and a deoxynucleotide-Fab complex. *Proteins* **11,** 159–175
21. Juri Ayub, M., Smulski, C., Nyambega, B., Bercovich, N., Masiga, D., Vazquez, M., Aguilar, C. F., and Levin, M. J. (2005) Protein-protein interaction map of the *Trypanosoma cruzi* ribosomal P protein complex. *Gene* **357,** 129–136
22. Matsumoto, S. C., Labovsky, V., Roncoroni, M., Guida, M. C., Gimenez, L., Mitelman, J., Gori, H., Jurgelevicius, R., Grillo, A., Manfredi, P., Levin, M. J., and Paveto, C. (2006) Retinal dysfunction in patients with chronic Chagas' disease is associated to anti-*Trypanosoma cruzi* antibodies that cross-react with rhodopsin. *FASEB J.* **20,** 550–552
23. Snary, D., Flint, J. E., Wood, J. N., Scott, M. T., Chapman, M. D., Dodd, J., Jessell, T. M., and Miles, M. A. (1983) A monoclonal antibody with specificity for *Trypanosoma cruzi,* central and peripheral neurones and glia. *Clin. Exp. Immunol.* **54,** 617–624
24. Sterin-Borda, L., Cantore, M., Pascual, J., Borda, E., Cossio, P., Arana, R., and Passeron, S. (1986) Chagasic IgG binds and interacts with cardiac beta adrenoceptor-coupled adenylate cyclase system. *Int. J. Immunopharmacol.* **8,** 581–588
25. Hernandez-Munain, C., De Diego, J. L., Alcina, A., and Fresno, M. (1992) A Trypanosoma cruzi membrane protein shares an epitope with a lymphocyte activation antigen and induces crossreactive antibodies. *J. Exp. Med.* **175,** 1473–1482
26. Hernandez-Munain, C., De Diego, J. L., Bonay, P., Girones, N., and Fresno, M. (1993) GP 50/55, a membrane antigen of *Trypanosoma cruzi* involved in autoimmunity and immunosuppression. *Biol. Res.* **26,** 209–218
27. Giordanengo, L., Maldonado, C., Rivarola, H. W., Iosa, D., Girones, N., Fresno, M., and Gea, S. (2000) Induction of antibodies reactive to cardiac myosin and development of heart alterations in cruzipain-immunized mice and their offspring. *Eur. J. Immunol.* **30,** 3181–3189
28. Lopez-Bergami, P., Cabeza Meckert, P., Kaplan, D., Levitus, G., Elias, F. Quintana, F., Van Regenmortel, M. H. V., Laguens, R., and Levin, M. J. (1997) Immunization with recombinant *Trypanosoma* cruzi ribosomal P2β protein induces changes in the electrocardiogram of immunized mice. *FEMS Immunol. Med. Microbiol.* **18,** 75–85
29. Sepulveda, P, Liegeard, P., Wallukat, G., Levin, M. J., and Hontebeyrie, M. (2000) Modulation of cardiocyte functional activity by antibodies against *Trypanosoma* cruzi ribosomal P2 protein C terminus. *Infect. Immun.* **68,** 5114–5119

30. Peter, J. C., Eftekhari, P., Billiald, P., Wallukat, G., and Hoebeke, J. (2003) scFv single chain antibody variable fragment as inverse agonist of the beta2-adrenergic receptor. *J. Biol. Chem.* **278,** 36740–36747
31. Peter, J. C., Wallukat, G., Tugler, J., Maurice, D., Roegel, J. C., Briand, J. P., and Hoebeke, J. (2004) Modulation of the M2 muscarinic acetylcholine receptor activity with monoclonal anti-M2 receptor antibody fragments. *J. Biol. Chem.* **279,** 55697–55706
32. Klco, J. M., Wiegand, C. B., Narzinski, K, and Baranski, T. J. (2005) Essential role for the second extracellular loop in C5a receptor activation. *Nat. Struct. Mol. Biol.* **12,** 320–326
33. Levin, M. J., Vazquez, M., Kaplan, D., and Schijman, A. G. (1993) The *Trypanosoma cruzi* ribosomal P protein family: classification and antigenicity. *Parasitol. Today* **9,** 381–384
34. Mesri, E.A., Levitus, G., Hontebeyrie-Joskowicz, M., Dighiero, G., Van Regenmortel, M. H., and Levin, M. J. (1990) Major *Trypanosoma cruzi* antigenic determinant in Chagas' heart disease shares homology with the systemic lupus erythematosus ribosomal P protein epitope. *J. Clin. Microbiol.* **28,** 1219–1224
35. Levitus, G., Hontebeyrie-Joskowicz, M., Van Regenmortel, M. H., and Levin, M. J. (1991) Humoral autoimmune response to ribosomal P proteins in chronic Chagas heart disease. *Clin. Exp. Immunol.* **85,** 413–417

Received for publication January 13, 2006.
Accepted for publication March 14, 2006.